Conformation-specific antibodies reveal distinct actin structures in the nucleus and the cytoplasm

ARTICLE *in* JOURNAL OF STRUCTURAL BIOLOGY · JANUARY 2006

Impact Factor: 3.23 · DOI: 10.1016/j.jsb.2005.09.003 · Source: PubMed

6 AUTHORS, INCLUDING:

Sabine Buchmeier
Technische Universität Braunschweig
12 PUBLICATIONS **511** CITATIONS
SEE PROFILE

Melanie Börries
German Cancer Research Center
35 PUBLICATIONS **696** CITATIONS
SEE PROFILE

Ueli Aebi
University of Basel
389 PUBLICATIONS **22,287** CITATIONS
SEE PROFILE

ARTICLE IN PRESS

Available online at www.sciencedirect.com
SCIENCE DIRECT®

Journal of Structural Biology xxx (2005) xxx–xxx

Journal of Structural Biology

www.elsevier.com/locate/yjsbi

Conformation-specific antibodies reveal distinct actin structures in the nucleus and the cytoplasm

C.-A. Schoenenberger [a,*], S. Buchmeier [b], M. Boerries [a], R. Sütterlin [a], U. Aebi [a], B.M. Jockusch [b]

[a] *M.E. Müller Institute for Structural Biology, Biozentrum, University of Basel, CH-4056 Basel, Switzerland*
[b] *Cell Biology, Zoological Institute, Technical University of Braunschweig, D-38092 Braunschweig, Germany*

Received 20 May 2005; received in revised form 2 September 2005; accepted 20 September 2005

Abstract

For many years the existence of actin in the nucleus has been doubted because of the lack of phalloidin staining as well as the failure to document nuclear actin filaments by electron microscopy. More recent findings reveal actin to be a component of chromatin remodeling complexes and of the machinery involved in RNA synthesis and transport. With distinct functions for nuclear actin emerging, the quest for its conformation and oligomeric/polymeric structure in the nucleus has resumed importance. We used chemically cross-linked 'lower dimer' (LD) to generate mouse monoclonal antibodies specific for different actin conformations. One of the resulting antibodies, termed 1C7, recognizes an epitope that is buried in the F-actin filament, but is surface-exposed in G-actin as well as in the LD. In immunofluorescence studies with different cell lines, 1C7 selectively reacts with non-filamentous actin in the cytoplasm. In addition, it detects a discrete form of actin in the nucleus, which is different from the nuclear actin revealed by the previously described 2G2 [Gonsior, S.M., Platz, S., Buchmeier, S., Scheer, U., Jockusch, B.M., Hinssen, H., 1999. J. Cell Sci. 112, 797]. Upon latrunculin-induced disassembly of the filamentous cytoskeleton in Rat2 fibroblasts, we observed a perinuclear accumulation of the 1C7-reactive actin conformation. In addition, latrunculin treatment led to the assembly of phalloidin-staining actin structures in chromatin-free regions of the nucleus in these cells. Our results indicate that distinct actin conformations and/or structures are present in the nucleus and the cytoplasm of different cell types and that their distribution varies in response to external signals.

Keywords: Actin antibody; Actin conformation; Latrunculin; Nucleus; Nucleocytoplasmic transport

1. Introduction

Actin has been characterized as an abundant protein with a plethora of diverse functions in the cytoplasm, but it has also been described as a component of the nucleus for quite some time (Bremer et al., 1981; Gonsior et al., 1999; Grenklo et al., 2004; Jockusch et al., 1974; Scheer et al., 1984). The failure to detect bona fide filaments that stain with phalloidin in nuclei conferred to many that nuclear actin simply reflects a contamination from the cytoplasm. However, recently the longstanding argument over the true existence of nuclear actin has been settled by the emergence of specific functions. For instance, it has been demonstrated that nuclear actin contributes to transcription by associating with initiation complexes of all three RNA polymerases, i.e., polymerase I (Philimonenko et al., 2004), II (Egly et al., 1984; Kukalev et al., 2005; Percipalle et al., 2003; Scheer et al., 1984; Smith et al., 1979), and III (Hu et al., 2004). In addition, evidence is increasing that nuclear actin is involved in the processing and export of mRNAs (Hofmann et al., 2001; Sahlas et al., 1993) and in chromatin remodelling (Olave et al., 2002; Percipalle et al., 2002; Rando et al., 2000). Notably, there is no evidence that conventional actin filaments, so abundantly present in the cytoplasm, are the building blocks of a nuclear matrix in tissue forming cells. In *Xenopus* oocytes, actin has been identified

* Corresponding author. Fax: +41 61 267 2109.
E-mail address: Cora-Ann.Schoenenberger@unibas.ch (C.-A. Schoenenberger).

1047-8477/$ - see front matter © 2005 Elsevier Inc. All rights reserved.
doi:10.1016/j.jsb.2005.09.003

as a component of a filamentous network that may be part of the nuclear matrix (Gonsior et al., 1999; Kiseleva et al., 2004). However, the conformation of actin in these structures is unknown.

Because of its diverse nuclear functions, actin cannot be considered a mere thermodynamic wanderer that transiently occupies the nucleus. Rather, the levels of actin in this cellular compartment have to be regulated. Although actin itself does not harbor a classical nuclear localization signal (NLS), some of the proteins that bind actin, for example cofilin, do. On the other hand, profilin and β4-thymosin that bind monomeric actin and are also present in the nucleus lack a classical NLS. With a molecular mass of 42,000 and a compact structure, actin, even in complex with small proteins like profilin, may well pass through the nuclear pores (Fahrenkrog and Aebi, 2003) by passive diffusion. With several active and passive pathways for entering the nucleus, it seems more likely that regulating its export from the nucleus controls the level of actin. Consistent with this notion, two conserved nuclear export signals (NESs) have been described for actin (Wada et al., 1998). More recently, exportin 6, a novel transport receptor of the importin-β superfamily, has been shown to mediate the nuclear export of profilin–actin complexes in higher eukaryotic cells (Stüven et al., 2003). Based on their findings, Stüven et al. suggested exportin 6 to function as a suppressor of actin polymerization in the nucleus.

As the data described above point to multiple, seemingly unrelated functions within the nucleus, nuclear actin might comprise actin in a number of different conformations. The association with RNA polymerases II and III is apparently restricted to β-actin (Hofmann et al., 2004; Hu et al., 2004) but there is no information on the other actin isoforms with respect to nuclear functions. The notion that nuclear actin does not exist in a filamentous, phalloidin-binding form prompted the speculation that it exists either as G-actin monomers or in unconventional conformations, such as very short polymers not containing the 'F-actin'-conformation, that specifically occur in the nucleus and are distinct from those found in conventional actin filaments in the cytoplasm.

To challenge this possibility, we have started to generate a panel of monoclonal antibodies recognizing specific actin conformations. Hereby, we consider even subtle spatial rearrangements of the actin molecule to represent a distinct conformation. We present comparative data on two of these antibodies, describing their reactivity and usefulness as tools to localize nuclear actin. Our data support the hypothesis that more than one form of actin exists in the nucleus of cultured cells.

2. Materials and methods

2.1. Cells

HeLa and Rat2 fibroblasts (Leavitt et al., 1985) were grown in Dulbecco's minimal essential medium supplemented with 2 mM L-glutamine, 100 IU/ml penicillin, 100 μg/ml streptomycin, and 10% FCS (DFCS) at 37 °C, in a humidified atmosphere containing 5% CO_2. Cells were subcultured weekly up to 10 passages.

2.2. Reagents

Latrunculin-A (LatA; Calbiochem) was stored as a 2 mM stock solution in DMSO at −70 °C. LatA was diluted to a final concentration of 5 μM in DFCS prior to use. Alexa Fluor 568-phalloidin was purchased from Molecular Probes. DRAQ5 cell permeant DNA probe was obtained from Alexis Biochemicals.

2.3. Antigens and antibodies

Purified actin isolated from skeletal rabbit muscle was covalently cross-linked at the onset of KCl-induced polymerization using homobifunctional 1,4-penylenebis maleimide (PBM; Sigma). A freshly prepared 5 mM PBM stock solution in dimethylformamide was diluted to 12 μM in 10 mM sodium borate, pH 9.2, containing 20 mM $CaCl_2$ immediately prior to use. For cross-linking, an equal volume of freshly diluted PBM was added to 24 μM G-actin solution in buffer A (2.5 mM imidazole, 0.2 mM $CaCl_2$, 0.2 mM DTT, 0.2 mM ATP, and 0.005% NaN_3, pH 7.4) immediately after the initiation of polymerization by 20 mM $CaCl_2$ to achieve a final molar ratio of 0.5:1 PDM/actin. After 15 min incubation at room temperature, further cross-linking was blocked by the addition of a tenfold molar excess of β-mercaptoethanol. After extensive dialysis against buffer A, cross-linked lower dimer (LD) was separated from monomeric actin by gel filtration chromatography using a Superdex 200 HiLoad column (Amersham Biosciences). Fractions containing <95% LD were pooled and concentrated by flow filtration.

The monoclonal antibody 1C7 was generated by immunizing mice with LD following a standard immunization protocol. After hybridization and cloning, antibody producing hybridoma cells were screened for their binding to LD and G-actin by ELISA. Isotype analysis of the strongly reactive clone 1C7 revealed it to be an IgG1 subtype. Supernatants were grown either according to standard protocols or in serum-free medium in the presence of 500 mg/L albumin and 10 mg/L transferrin. 1C7 was used as culture supernatant or purified by immunoaffinity chromatography using anti-mouse IgG-agarose (Sigma).

Production and purification of monoclonal anti-actin 2G2 (IgM) has been described previously (Gonsior et al., 1999).

2.4. Dot blot analysis

Serial dilutions of purified protein (rabbit skeletal muscle G-actin, LD, BSA) in buffer A were applied onto a PVDF immobilon-P membrane by vacuum filtration in a

blotting unit. Membranes were removed from the blotting unit and incubated in 5% milk/PBS containing 0.05% Tween 20 (PBS-T) without allowing them to dry. Dot blots were incubated with primary antibodies for 1 h at 37 °C, washed with 5% milk/PBS-T, PBS-T, 1% Blotto in PBS-T, and then with a 1/10 000 dilution of an alkaline phosphatase-conjugated anti-mouse Ig (Sigma). CDP-star (Tropix) was used as substrate to develop dot blots.

2.5. Pepscan analysis

For the identification of 1C7-reactive amino acid residues, the sequence of the reactive proteolytic actin fragment was spot-synthesized on cellulose membranes as peptides of 15 aa in length with an overlap of 12 aa (Frank, 2002). 1C7-binding to this sequence on the membrane was monitored as described by Mayboroda et al. (1997).

2.6. Immunofluorescence

For immunofluorescence, cells were grown on glass coverslips for 24–48 h to subconfluency. Coverslips were rinsed twice with PBS before fixation. Different fixation protocols were used as indicated. Cells were either fixed for 10 min with freshly prepared 3% paraformaldehyde in PBS, for 15 min with formalin solution (Sigma), or for 15 min with −20 °C MeOH. In some cases, cells were extracted for 5 min with 2% octyl-POE (*n*-octylpolyoxyethylene, Alexis) in modified Hanks' buffer (MHB; Small and Celis, 1978) containing 0.12% glutaraldehyde prior to fixation by 1% glutaraldehyde for 20 min (Baschong et al., 2001). After several washes in MHB, aldehyde groups were quenched by two times 10 min incubations with 0.5 mg/ml $NaHB_4$ in MHB on ice.

Appropriate dilutions of the primary antibodies 1C7 and 2G2 were incubated for 1 h at room temperature (RT) or overnight at 4 °C in a humidified chamber. The following primary antibodies were also used for immunostaining: mouse monoclonal anti-actin C4 (10 μg/ml; Chemicon International) and polyclonal guinea pig anti-human emerin (1/300; kindly provided by H. Herrmann-Lerdon, DKFZ Heidelberg). After several washes in PBS, coverslips were placed on a drop of the corresponding secondary antibody solution and incubated for 1 h at RT. Secondary antibodies used were Alexa Fluor 488-conjugated anti-mouse IgG (H and L chain, Alexis; 1/800) and FITC-conjugated goat anti-mouse IgM (μ-chain specific, Sigma; 1/100) and Cy5-conjugated anti-guinea pig IgG (Jackson ImmunoResearch Laboratories; 1/300). In some cases, Alexa Fluor 568-phalloidin (1/250; Molecular Probes) and/or DRAQ5 (1/250; Alexis Biochemicals) were incubated together with the secondary antibody. Confocal images were obtained using a 63× or 100× oil objective on a Leica TCS SP laser scanning confocal microscope. Digitized confocal images were processed by Leica software, Imaris 4.1 (Bitplane AG) and Adobe Photoshop.

2.7. Immunoelectron microscopy

Trypsinized HeLa cells were pelleted, washed once with PBS, and immediately fixed for 1 h at 4 °C in Karnowski fixative (0.5% glutaraldehyde and 3% paraformaldehyde in 10 mM phosphate buffer, 85.5 mM NaCl, and 20 mM NaN_3, pH 7.4). Fixed cells were pelleted and embedded in 2% agar. Specimens were dehydrated in ethanol and subsequently embedded in LRW (Polysciences, USA). Ultrathin sections were mounted on carbon/parlodion-coated copper grids and grids were blocked in 2% BSA in PBS two times 5 min before incubation with 1C7 and 2G2 antibodies for 2 h at RT. Grids were washed in PBS and blocked in 2% BSA in PBS for two times 5 min before incubating them with 10 nm gold-conjugated goat anti-mouse IgM (μ-chain specific) or anti-mouse IgG secondary antibodies (BBInternational) for 1 h. After washing in PBS and water, grids were treated with a mixture of 6% uranyl acetate for 1 h, rinsed with water and then post-stained for two minutes with lead-citrate. Micrographs were recorded with a Hitachi 7000 at 80 kV.

3. Results

3.1. Characterization of actin antibodies

To produce monoclonal antibodies that recognize distinct forms of actin, we immunized mice with an unconventional actin structure. Specifically, we used a chemically cross-linked actin dimer, the 'lower dimer' (LD; Millonig et al., 1988) as immunogen. The LD is transiently formed at the onset of actin polymerization, but appears to be absent in F-actin filaments at steady state (Elzinga and Phelan, 1984; Millonig et al., 1988; Mockrin and Korn, 1981). By covalently cross-linking the LD with *N*,*N*′-*p*-phenylenebismaleimide (PBM), this particular actin conformation could be fixed, biochemically isolated, and used for immunization.

Monoclonal antibodies were detected in ELISA analyses, using G-actin from rabbit skeletal muscle and PBM cross-linked LD. Isotyping of positive clones revealed that the vast majority of clones were producing IgMs. Anticipating some adverse effects in using the large pentameric structure of IgMs, we focused on those clones producing IgGs. One of these clones produced antibodies of the IgG1 subclass that is referred to as 1C7. 1C7 was characterized in detail and compared to the previously reported monoclonal 2G2, an IgM which was raised against a profilin:actin complex and recognizes a particular nuclear actin conformation present in certain cell types (Gonsior et al., 1999). In contrast to the 2G2 antibody, 1C7 reacted only poorly with SDS-denatured purified actin or actin in total cell extracts on Western blots (data not shown). When serial dilutions of purified actin or cross-linked LD were directly applied to the membrane under non-denaturating conditions, 1C7 bound to monomeric actin as well as to LD (Fig. 1A). With comparable amounts of protein, the intensity of the signal

was similar for both antigens. In this assay, 2G2 also bound to actin and LD with similar intensity.

The epitope recognized by 1C7 was identified by pepscan analysis (Frank, 2002). As shown in Fig. 1B, a series of 37 synthetic peptides that correspond to the actin sequence aa 104–227 was synthesized on the membrane. Each peptide comprised 15 amino acids, with an overlap of 12 residues between adjacent peptides. After incubation of the membrane with 1C7, clear positive signals were obtained with peptides 29, 30, and 31. Taking into consideration the 12 aa overlap, we concluded that only those residues shared between the three adjacent 1C7-reactive peptides (i.e., TERGYSFVTT) contributed to the epitope. These regions correspond to residues aa 194–203, which are identical in skeletal muscle and cytoplasmic actin of rabbit, rat, and man. To reveal the topography of the 1C7-epitope, the reactive residues were displayed in space filling mode within the ribbon structure of monomeric actin (Fig. 1C). The 1C7 epitope comprises a linear sequence of a loop with no distinct secondary structure, which connects two helices in actin subdomain 4 (magenta, top panel). This topology is clearly distinct from that of the 2G2 epitope (green, bottom panel), which consists of three interspersed patches. Moreover, the entire epitope recognized by 1C7 is exposed on the surface of subdomain 4, whereas parts of the 2G2 epitope are buried within the molecule. Mapping the epitope onto the crystallographic structure of an antiparallel actin dimer as reported by Bubb et al. (2002; right panel), where the subunit orientation is similar if not identical to that of LD, revealed that the 1C7 epitope is surface-exposed and thus accessible for antibody binding on both subunits.

3.2. 1C7 recognizes only non-filamentous actin in cells

To determine the cellular localization of the 1C7 epitope, we stained different cell lines by indirect immunofluorescence and compared the staining pattern of 1C7 to that of 2G2 and that of phalloidin-positive filamentous actin. We used two different cell lines: rat fibroblasts (Rat2), as these spread well and establish an extensive network of actin stress fibers, and HeLa cells which compared to the cell volume have a relatively large nucleus. In Rat2 (Fig. 2A) or HeLa cells (Fig. 2B) fixed with 3% paraformaldehyde and then permeabilized with 0.2% Triton X-100, 1C7 showed a fine disperse, slightly punctate labeling throughout the cell. In particular, there was a significant amount of labeling in the nucleus except for the nucleoli. Overlaying the staining pattern of phalloidin (Figs. 2A′ and B′; red) with 1C7 (green) revealed that most of the actin recognized by 1C7 did not co-localize with filamentous actin. This finding

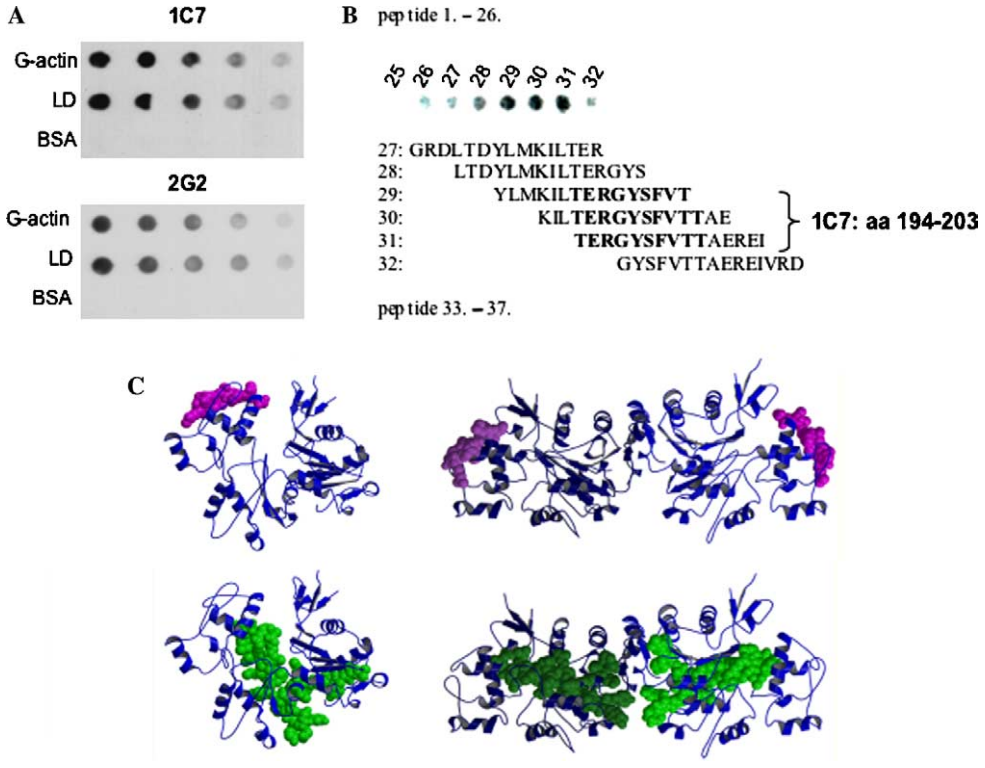

Fig. 1. The 1C7 antibody recognizes a consecutive sequence on the surface of actin. (A) Dot blot analysis with 4-fold serial dilutions of purified G-actin, cross-linked lower dimer (LD, see text), and bovine serum albumin (BSA), starting at 500 ng. 1C7 and the previously characterized monoclonal antibody 2G2 (Gonsior et al., 1999) both react with monomeric actin as well as with the cross-linked LD. (B) Pepscan analysis of 1C7 reactivity using 37 peptides (15 aa each) that correspond to aa 104–226 of the actin sequence with 12 aa overlap between consecutive peptides. The 10 aa shared by 1C7 reactive peptides 29, 30, and 31 comprise the 1C7 epitope (bold). They correspond to aa 194–203 of the rabbit skeletal muscle actin. (C) Comparison of 1C7 and 2G2 binding epitopes. The epitopes of 1C7 (magenta) and 2G2 (green) determined by pep scan analysis are fitted in a space filling mode on the ribbon model of monomeric actin (Kabsch et al., 1990) on the left, and on the structure of an antiparallel actin dimer (Bubb et al., 2002) on the right.

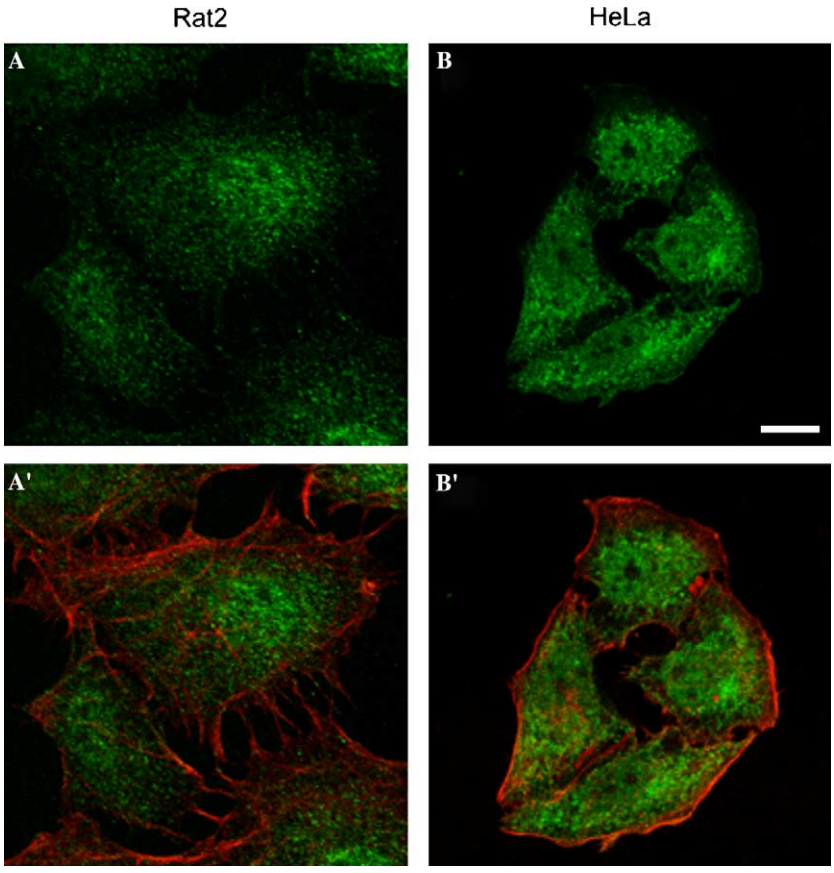

Fig. 2. Cellular localization of the 1C7 actin epitope. In Rat 2 (A) and HeLa (B) cells that were fixed with 3% paraformaldehyde and permeabilized with 0.2% Triton X-100, 1C7 exhibits a fine disperse staining (green) with a decreasing intensity towards the cell periphery. Except for the nucleoli, the nuclei are also labeled. (A′, B′) Counterstaining of the cells shown in (A, B) with 568-phallodin (red) reveals little co-localization between filamentous actin and the actin conformation binding 1C7.

indicated that 1C7 reacts with a specific actin conformation. The staining pattern obtained with cells that had been microinjected with 1C7 confirmed this interpretation (data not shown). When cells were extracted with octyl-POE prior to fixation with 1% glutaraldehyde (Fig. 3), the fine disperse staining with 1C7 persisted in the cytoplasm. However, the nuclear structures were apparently removed by the detergent treatment, indicating that the staining pattern obtained with 1C7 was fixation-dependent.

By comparing the staining patterns obtained for 1C7 (Figs. 3A and B) and 2G2 (Figs. 3C and D) with identical fixation protocols, it became evident that the overall images obtained with 1C7 and 2G2 differed: while 1C7 revealed a more homogenous dispersion of fine dots throughout the cytoplasm, 2G2 displayed mostly nuclear actin in fewer, but prominent dots (Figs. 3C and D).

In both, cells pre-extracted with octyl-POE before fixation as well as in cells fixed with 3% paraformaldehyde or formalin prior to extraction, 1C7 did not label actin filaments. Similarly, 2G2 labeling under these conditions showed no co-localization with phalloidin-stained filamentous actin (Figs. 3C and D). However, it had been shown previously that 2G2 decorates stress fibers in fibroblasts after fixation and extraction with cold methanol (Gonsior et al., 1999). To examine whether such a rather drastic denaturation similarly exposes the 1C7 epitope on stress fibers, we fixed Rat2 cells with cold MeOH and reacted them with different actin antibodies (Fig. 4). Under these conditions, a typical stress fiber staining was observed with a commercially available monoclonal actin antibody (Fig. 4A) as well as with 2G2 (Fig. 4B). In contrast, 1C7 still exhibited a fine punctate staining throughout the cells and no filamentous staining pattern (Fig. 4C). In Figs. 4D and 3E, we superimposed a ribbon representation of three neighboring actin subunits in the Holmes–Lorenz filament model (Holmes et al., 1990; Lorenz et al., 1993) with the epitope sequence indicated in red onto a corresponding volume-rendered model of the F-actin filament. In this representation the end-on view (Fig. 4D) as well as the side-view (Fig. 4E) show that the epitope sequence (i.e., aa 194–203) is indeed buried within the filament and may thus remain inaccessible to 1C7 even after methanol denaturation.

3.3. The actin conformation recognized by 1C7 is present in the nucleus

The data described above indicate that nuclear actin as recognized by 1C7 is predominantly or entirely non-filamentous. We examined this possibility further, by

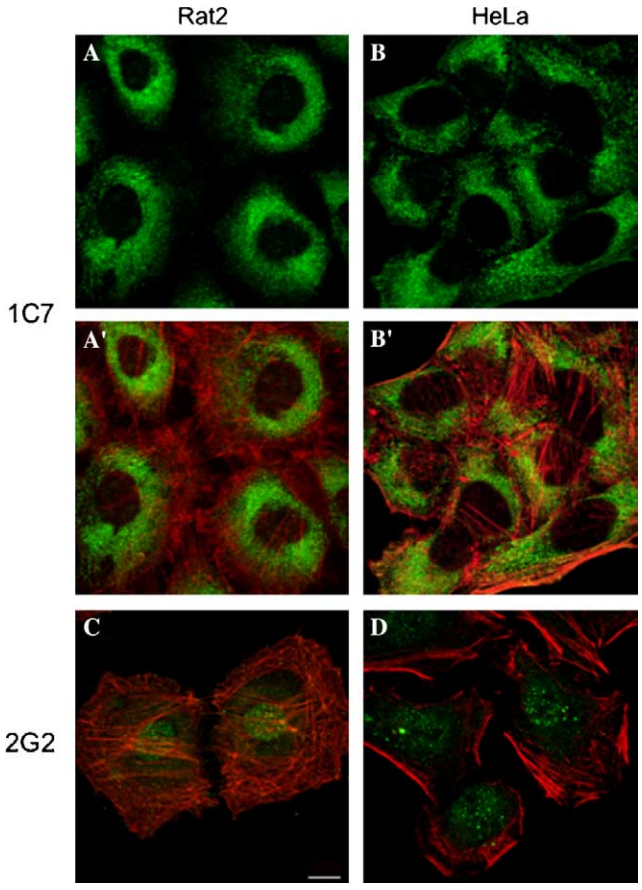

Fig. 3. 1C7 and 2G2 recognize different actin populations. Confocal sections through Rat2 fibroblasts (left column) and HeLa cells (right column) immunostained with 1C7 (A, B) or 2G2 (C, D) are shown. Cells were extracted with 2% octyl-POE in MHB (see Section 2) prior to 1% glutaraldehyde fixation. (A, B) This treatment largely abolished the nuclear staining in 1C7-labeled cells. A slight concentration of the punctate 1C7 staining in the perinuclear area is seen. (A′, B′) Counterstaining of the cells shown in (A, B) with 568-phallodin (red) reveals little co-localization between filamentous actin and the actin conformation binding 1C7. (C, D) Cells fixed as in (A, B), but labeled with 2G2 (green) and 568-phallodin. The actin conformation detected by 2G2 is predominantly nuclear and does not co-localize with phalloidin-positive actin stress fibers. Bar, 10 μm.

studying the localization of the actin conformation seen by 1C7, by confocal laser scanning microscopy of immunolabeled cells and by immuno EM. Fig. 5A shows an optical section through HeLa cells taken at the level of the nucleus, as identified by the DNA staining with Draq5 (blue). The optical section revealed a dot-like labeling of structures in the nucleus. These nuclear dots were predominantly located at sites free of chromatin. The nuclear localization of 1C7-reactive actin was confirmed in a double labeling experiment using a polyclonal antibody against emerin (Dreger et al., 2002), a key component of the nuclear envelope. As expected and illustrated in Fig. 5B, the emerin antibody (blue) delineated the nuclear compartment by revealing the nuclear envelope. At this sectional plane taken through the cell, the actin conformation recognized by 1C7 was found abundant within the boundaries of the nucleus as well as in the cytoplasm. Except for the nucleoli, 1C7 labeling was seen rather evenly distributed throughout the nucleoplasm (Fig. 5B). In contrast to the actin conformation recognized by 1C7, 2G2 detected an actin conformation that was predominantly localized in dot-like structures in the nucleus (Fig. 5D) of cells fixed with 10% neutral-buffered formalin and permeabilized with Triton X-100.

Extraction of cells with octyl-POE/0.1% glutaraldehyde in MHB before fixation with 1% glutaraldehyde (Fig. 5E) unveiled additional binding sites for 2G2 at the cell periphery, in particular in filopodia extending from the cell border. Notably, this peripheral 2G2 labeling did not co-localize with phalloidin-positive actin. A similar pattern was observed when the cells were first stained with fluorescent phalloidin followed by incubation with 2G2, indicating that the absence of phalloidin staining was not caused by binding of the IgM antibody (data not shown).

To investigate the in situ localization of the 1C7 actin conformation in the nucleus at higher resolution, we carried out post-embedding immunogold labeling of ultrathin sections of HeLa cells at the EM level. This technique offers the advantage that variations in the actin distribution related to permeabilization/extraction procedures are avoided. Fig. 5C illustrates that 1C7-conjugated gold particles were detected in the cytoplasm and nucleoplasm. Consistent with the immunofluorescence labeling, we neither observed an association of gold particles with discrete nuclear structures nor an increased density of gold particles at the nuclear envelope.

Fig. 5. 1C7 and 2G2 detect different actin populations in the nucleus. (A) HeLa cells were fixed with 10% neutral-buffered formalin solution, permeabilized with 0.2% Triton X-100, and then labeled by indirect immunofluorescence with 1C7 actin antibody (green). DNA was identified with DRAQ5 (blue). The confocal section through the nucleus reveals a dot-like labeling of structures in the nucleus besides the dispersed, fine punctate staining in the cytoplasm. Dots are predominantly located at chromatin-free sites. (B) Immunofluorescence of HeLa cells fixed in 3% paraformaldehyde/PBS and extracted with −20 °C MeOH. Cells were double-labeled with monoclonal 1C7 actin antibody (green) and a polyclonal emerin antibody (blue). The confocal section at the height of the nucleus reveals a pronounced nuclear rim staining for emerin. 1C7 staining is evenly distributed throughout the cytoplasm, as well as the nucleus. Areas corresponding to nucleoli do not bind 1C7. Bar, 10 μm. (C) Post-embedding immunogold labeling of ultrathin sections of HeLa cells with 1C7 confirms that the actin conformation recognized by 1C7 is present in the cytoplasm (c) and the nucleus (n). (D) Confocal section at the level of the nucleus of HeLa cells fixed and permeabilized as in (A). Cells were labeled with 2G2 by indirect immunofluorescence (green) and counter stained with DRAQ5 (blue). Under these conditions, 2G2 predominantly labels dot-like structures in the nucleus. Bar, 10 μm. (E) HeLa cells were extracted with octyl-POE/0.1% glutaraldehyde in MHB before fixation with 1% glutaraldehyde. In addition to nuclear actin, 2G2 binding sites at the cell periphery and in filopodia extending from the periphery are unveiled by this protocol. Counterstaining with Alexa 568-phalloidin reveals that 2G2 does not bind to stress fibers. Bar, 10 μm. (F) Post-embedding immunogold labeling of ultrathin sections of HeLa cells with 2G2 confirms that the actin conformation recognized by 2G2 is abundant in the nucleus (n), but a few gold particles are also seen in the cytoplasm. Bar, 100 nm.

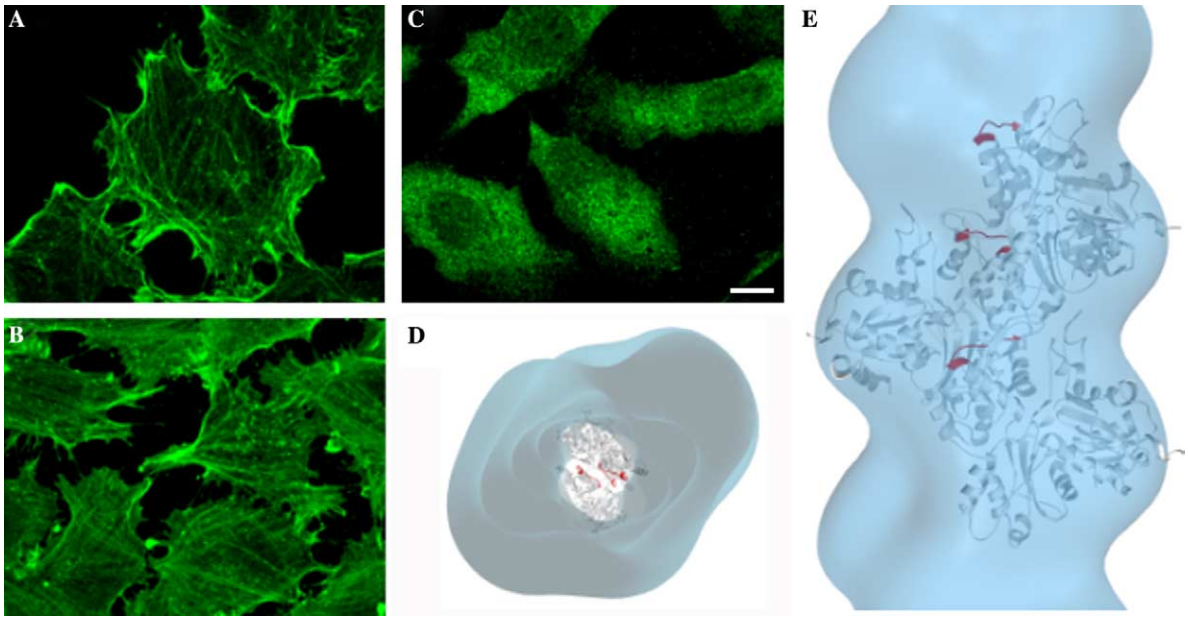

Fig. 4. 1C7 does not react with filamentous actin. (A–C) Immunofluorescence labeling of Rat2 cells fixed with −20 °C MeOH. (A) Monoclonal C4 actin antibody reacts with stress fibers. (B) MeOH treatment reveals the 2G2 epitope on cytoplasmic actin bundles, whereas nuclear dot staining is eliminated. (C) The fine punctate staining pattern of 1C7 throughout the cytoplasm and nucleus is unaltered by MeOH denaturation. Bar, 10 μm. (D) End-on view into the Holmes–Lorenz model of an F-actin filament with the ribbon representation of three neighboring actin subunits fitted into the electron density iso-surface of the filament. The respective epitope sequences (aa 194–202) are highlighted in red. They are buried in the filament. (E) An averaged and refined 3-D helical reconstruction computed from negatively stained F-actin filament stretches, which has been surface-rendered to include 100% of its nominal molecular mass, was interactively fitted onto the ribbon representation of an actin trimer. The 1C7 epitope is indicated (magenta).

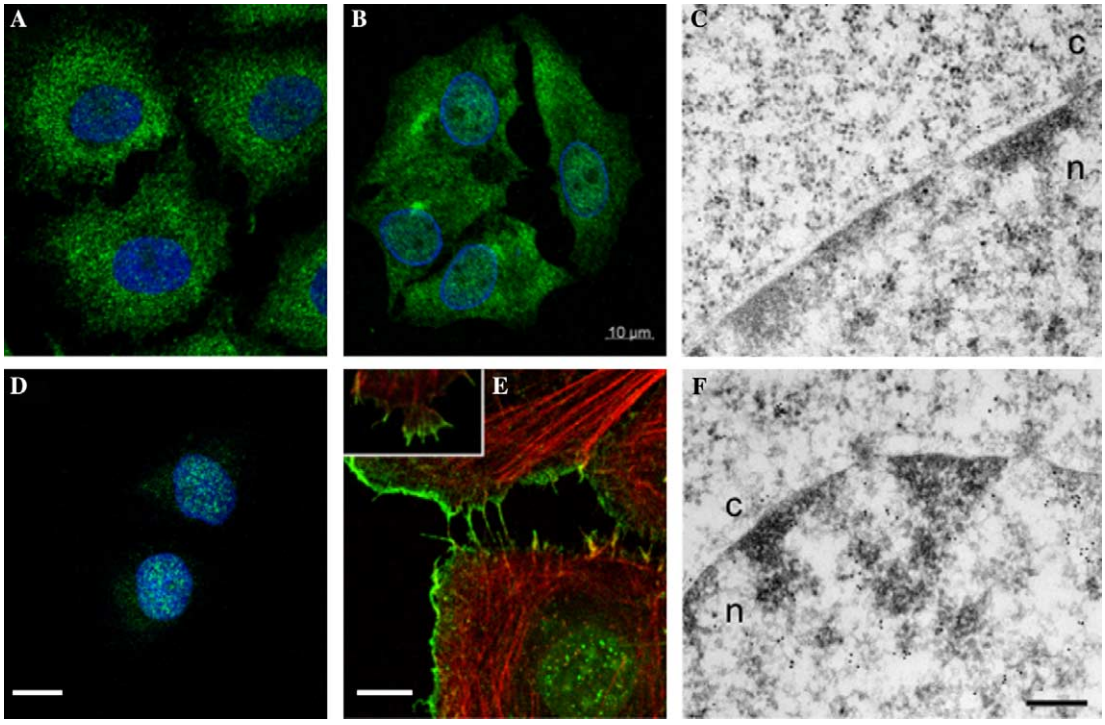

Immunogold labeling of HeLa sections with 2G2 confirmed that binding sites for this antibody were accumulated in the nucleus and significantly fewer gold particles were detected in the cytoplasm (Fig. 5F). Despite this rather dense nuclear labeling, we could not identify specific structures with which 2G2 preferentially associated. The slight clustering of gold particles in some areas might be due to the pentameric structure of the 2G2 antibody, causing reaction clusters, rather than to a local accumulation of the epitope.

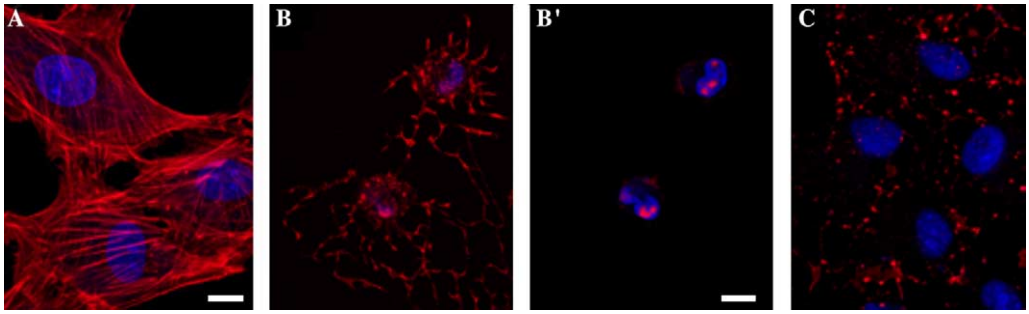

Fig. 6. The nucleus of LatA-treated Rat2 cells contains a phalloidin-positive actin conformation. (A) Untreated Rat2 fibroblasts display 568-phalloidin-positive stress fibers. Bar, 10 μm. (B) Incubation of Rat2 cells with LatA leads to the disassembly of stress fibers. An optical section near the substrate reveals remnants of 568-phalloidin-positive actin filament bundles in the cytoplasm. Nuclei are rounded up. (B′) An optical section at the height of the nuclei shows that a phalloidin-positive actin species has accumulated at discrete sites within the nucleus. Bar, 10 μm. (C) In LatA-treated HeLa cells, the residual 568-phalloidin F-actin cytoskeleton is more punctate. There are individual small dots but no larger aggregates of 568-phalloidin-positive actin in the nucleus. DNA was identified with DRAQ5 (blue) in all panels.

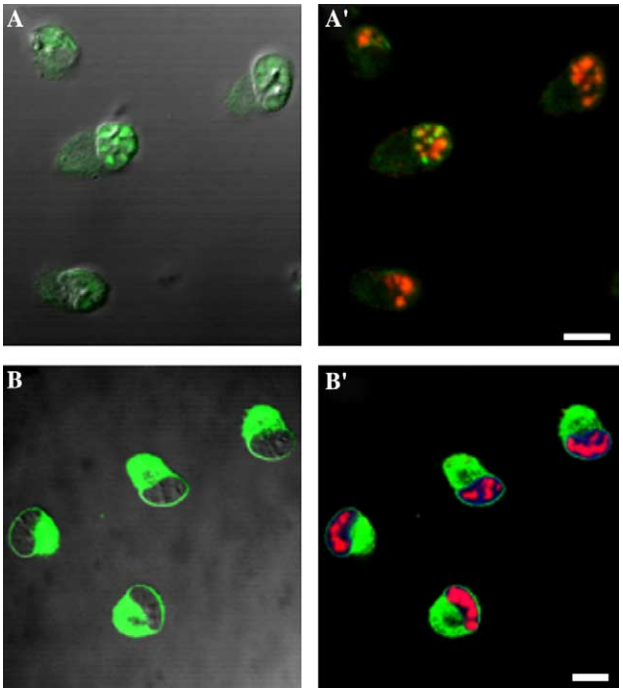

Fig. 7. 2G2 and 1C7 reveal distinct LatA-induced actin conformations. (A) Super-imposing the 2G2 labeling (green) on the DIC image shows that the nuclear actin conformation recognized by 2G2 forms large aggregates in Rat2 nuclei upon LatA treatment. (A′) The actin conformation detected by 2G2 (green) only partially overlaps with the 568-phalloidin-positive actin pool in the nucleus. (B) The cytoplasmic actin conformation recognized by 1C7 (green) translocates towards the nucleus and the nuclear rim is also labeled. However, there is no increased labeling of actin in the nucleus. (B′) 568-phalloidin-positive actin accumulates in the nucleus of LatA-treated Rat2 cells. Bar, 10 μm.

3.4. Latrunculin induces an increase in distinct nuclear actin conformations

Latrunculin-A (LatA) reversibly disrupts the cytoskeleton by binding to monomeric actin, thereby preventing it from repolymerizing into filaments ((Morton et al., 2000), Fig. 6). A translocation of actin, most of which does not bind phalloidin, to the nucleus was observed in mast cells after LatA treatment (Pendleton et al., 2003). This prompted us to investigate the effect of LatA on actin conformations in fibroblasts and epithelial cells. Fig. 6 illustrates the effects of LatA on the phalloidin-positive actin cytoskeleton in Rat2 fibroblasts. When cells were incubated for 3 h at 37 °C with 50 μM LatA and subsequently extracted and fixed with octyl-POE/glutaraldehyde, the phalloidin-positive cytoskeleton had largely disintegrated (Figs. 6B and B′). As shown by the optical section through the cell near the substrate (Fig. 6B), the original stress fibers had collapsed and only remnants were stained by phalloidin. At the height of maximal nuclear dimensions (Fig. 6B′), there was very little cytoplasmic actin stained by phalloidin. Instead, actin had accumulated in a phalloidin-positive conformation in the nucleus, predominantly in chromatin-free areas.

Under the same experimental conditions, cytoskeletal remnants in HeLa cells displayed a different appearance. The projection of optical sections through LatA-treated HeLa cells (Fig. 6C) revealed patches of phalloidin-positive actin at the cell periphery. Occasionally, we detected small dots of phalloidin-stained actin in the nucleus. However, these nuclear dots were much smaller than the phalloidin-positive actin structures in LatA-treated fibroblasts.

3.5. 1C7 and 2G2 reveal different LatA-induced actin conformations

Our data show that the two antibodies, 1C7 and 2G2, label different actin conformations with a distinct distribution pattern in the cytoplasm and the nucleus. We therefore tested whether such differences were also obvious after LatA treatment. Fig. 7A shows that after LatA treatment of Rat2 cells, the 2G2-reactive conformation is indeed present in large aggregates in the nucleus. When cells were simultaneously labeled with 568-phalloidin and 2G2 and the two channels merged (Fig. 7A′) it became evident that the 2G2-labeled actin conformation only partially overlapped with the phalloidin-positive actin in the nucleus. This finding indicates that at least two different nuclear actin conformations exist in Rat2 cells after LatA treatment.

Fig. 7B shows an optical section of 1C7-labeled Rat2 cells at the height of the nucleus, which had apparently compacted upon LatA treatment. The actin conformation labeled by 1C7 was abundant in the presence of LatA, suggesting a translocation of this species towards the nucleus. In addition, a distinct rim staining surrounding the nucleus was observed. Simultaneous labeling with an anti-lamin antibody confirmed the presence of the 1C7 epitope at the nuclear envelope (data not shown). In contrast to the accumulation of a phalloidin-positive actin species in the nucleus of Rat2 cells after LatA treatment, we did not observe any significant nuclear translocation of the 1C7 actin moiety (Fig. 7B′).

4. Discussion

4.1. Monoclonal antibodies detect different actin conformations

In this study, we describe a monoclonal actin antibody called 1C7, which selectively binds to cellular actin in a non-filamentous conformation. 1C7 was initially selected by its reactivity with a mixture of native G-actin and cross-linked LD in an ELISA. The actin conformation detected by 1C7 is abundant in the cytoplasm, but is also present in the nucleus of different cell types. Unlike other actin antibodies, such as 2G2 (Gonsior et al., 1999 and Fig. 4) and a recently published polyclonal antibody raised in chicken (Grenklo et al., 2004) which exhibit a filamentous staining pattern after methanol treatment, 1C7 did not bind to filamentous actin under these conditions. Even a mild detergent extraction prior to fixation did not reveal a filamentous staining pattern. Immuno EM with synthetic F-actin filaments and cosedimentation assays of 1C7 with prepolymerized actin filaments confirmed the absence of filament binding (data not shown). There are two possible explanations for the absence of filament binding: either actin subunits assembled into filaments cannot assume this particular conformation or the epitope is not accessible to the antibody. Consistent with the notion that a specific conformation of actin is required to bind 1C7, the antibody poorly reacted with SDS-denatured actin in Western blots. When denaturation was kept minimal by directly applying purified actin to a membrane in a dot blot assay, 1C7 bound as efficiently as 2G2 to both G-actin and cross-linked LD. A 10 amino acid sequence was identified as the 1C7 epitope. This sequence is present on the surface of subdomain IV in monomeric actin and also seems readily accessible in an antiparallel actin dimer (Bubb et al., 2002; Reutzel et al., 2004), the structure of which may be similar to that of cross-linked LD. The linear epitope is clearly distinct from the non-sequential epitope mapped for 2G2. Consistently, the two antibodies can distinguish between actin populations present in different conformational states.

Unmasking of epitopes by specific fixation/permeabilization protocols is not unusual, and has also been found for 2G2. As the 1C7-reactive sequence is not only buried in the filament (Fig. 4D) but is also involved in subunit–subunit interactions along and between axial strands, we cannot rule out that it remains inaccessible to the antibody in all fixation/permeabilization protocols employed. Since the F-actin conformation specifies a particular filamentous subunit arrangement we cannot unambiguously determine whether the epitope is physically inaccessible to the antibody or whether 1C7 does not bind to the F-actin conformation.

4.2. Different actin populations exist within the nucleus

1C7 differs from 2G2 not only with respect to the epitope recognized, but the actin populations revealed by these two antibodies also vary with respect to their cellular location. Depending on the cell type and the fixation/permeabilization protocol, 2G2 typically displays a pronounced nuclear dot-like staining pattern. The large size of the aggregates may in part be attributed to the pentameric nature of the IgM antibody. In case of a mild detergent extraction prior to fixation with glutaraldehyde, we observed that the filopodial tips at the cell periphery reacted with 2G2 but failed to bind phalloidin. 1C7 predominantly recognized non-filamentous actin in the cytoplasm but also clearly stained an actin conformation within the nuclear compartment. The fine punctate staining pattern revealed by 1C7 in the nucleus was quite different to the large nuclear dots stained by 2G2 under the same conditions. A comparison of the 1C7 epitope with the nuclear actin-related protein (Arp) sequences (Kato et al., 2001) showed that it was unique to actin and, therefore, the reactivity of 1C7 with nuclear constituents cannot be due to cross-reactivity with nuclear Arps (data not shown). Our findings indicate that actin in the nucleus exists in different conformations. A number of studies support this notion: for example, overexpression of cofilin leads to an accumulation of cofilin and actin in rod-like structures in the nucleus, suggesting that cofilin actively participates in the import of actin into the nuclear compartment (Yahara et al., 1996) and/or possibly its export from the nucleus. Phalloidin staining was absent in these structures, indicating that cofilin-associated structures did not represent conventional F-actin filaments. In addition, nuclear actin is also present as an actin–profilin complex (Stüven et al., 2003). Profilin-binding is known to cause significant changes in the actin conformation (Schutt et al., 1993). Moreover, the binding of actin to profilin markedly increased the efficiency of exportin 6-mediated nuclear export of actin in higher eukaryotic cells (Stüven et al., 2003). The assumption that at least two different actin conformations exist, one of them induced and stabilized by profilin and another one by cofilin, might also explain why Wada and co-workers found the two nuclear export signals (NES) in the actin sequence to be significant for its export out of the nucleus, whereas Stüven et al. reported the NES-mediated export pathway to be ineffective in their system. Because the immunogen used to produce 2G2 mAb was a

profilin–actin complex (Gonsior et al., 1999), it is conceivable that the dot-like structures labelled by 2G2 in the nuclei of certain cell types represents a 'profilin-induced' actin conformation.

Immuno-electron microscopy confirmed the presence of intranuclear 1C7 and 2G2-reactive actin species, but an association with discrete nuclear structures was not evident either in post-embedding labelling experiments (Fig. 5), nor in pre-embedding labelling experiments with isolated nuclei (data not shown). An association of actin with a heterogeneous filament network within the nucleus of *Xenopus* oocytes was recently documented by field emission scanning electron microscopy (Kiseleva et al., 2004). This network collapsed in the presence of LatA, and additional proteins such as protein 4.1 are essential components of this filamentous supramolecular assembly. However, the conformation and oligomerization/polymerization state of the actin residing in this network remain undetermined.

4.3. The conformation and amount of actin in the nucleus can be modulated by latrunculin

It has been known for nearly three decades that large amounts of actin are present in the nuclei of amphibian oocytes (Clark and Merriam, 1977). However, even in these nuclei conventional actin filaments could not be demonstrated, despite actin concentrations way above the critical concentration for polymerization into F-actin filaments. As already mentioned, nuclei of vertebrate somatic cells also lack phalloidin-stainable F-actin filaments under physiological conditions. In contrast, maturating spores of *Dictyostelium discoideum* naturally contain nuclear actin rods (Sameshima et al., 1994). These are composed of closely packed bundles of laterally aligned actin filaments with the same polarity that stained with phalloidin (Sameshima et al., 2001). In vertebrate cells, accumulation of actin in the nucleus and phalloidin-stainable structures could be induced by stress, such as treatment with DMSO (Sanger et al., 1980) or heat shock (Welch and Suhan, 1985). Actin accumulating in intranuclear rods has also been described in actin mutation-related actinopathies (Goebel and Warlo, 2001). Whether this actin represents wild type or mutated actin has not been determined. Expressing the nemaline myopathy mutant actin V163L in NIH3T3 fibroblasts resulted in rods and aggregates of mutant actin, some of which were located in the nucleus and co-stained with phalloidin (Clarkson et al., 2004). Together these findings suggest that rod-like accumulations of F-actin in the nucleus primarily occur when the amount of actin is imbalanced in the cytoplasmic and/or nuclear compartments. Consistently, depletion of Exp6 by RNA silencing also led to actin rods in the nucleus (Stüven et al., 2003).

When we treated Rat2 cells with LatA, we also observed a translocation of actin to the chromatin-free regions of the nucleus concomitant with the disassembly of cytoplasmic microfilaments. In these cells, a large fraction of the translocated actin was stained with phalloidin indicating that F-actin containing structures were assembled inside the nucleus. The filamentous nature of these structures was corroborated by the absence of 1C7 labelling in the nucleus. Moreover, the assembly of F-actin structures was reversible (data not shown). In contrast, increasing the cellular G-actin through latrunculin B treatment caused a nuclear translocation of actin in rat peritoneal mast cells, most of which was not stained by phalloidin (Pendleton et al., 2003). In this system, the actin was translocated in complex with cofilin, which may have prevented it from forming filaments, as outlined above. Consistently, nuclear rods that have been induced by cofilin overexpression contain actin that was not stained by phalloidin (Nishida et al., 1987). The phalloidin-positive actin, induced by Lat treatment, cannot be a general phenomenon, as we did not observe it in HeLa cells under the same experimental conditions.

5. Conclusions

The results presented in this report data clearly document that there are different conformations and oligomerization/polymerization states of actin present in the nucleus of different cell types. Moreover, nuclear actin conformations are dynamic and may change in response to cellular signals. It will be interesting to test whether different levels of exportins are correlated with the different actin conformations in the nucleus of different cell types. To challenge this and related questions, further monoclonal actin antibodies will be necessary as specific tools to probe for defined actin conformations. These might be generated by using specific conformations and/or oligomeric/polymeric states of actin as antigens.

Acknowledgments

We gratefully acknowledge the help of Daniel Stoffler (ME. Müller Institute for Structural Biology, University of Basel, Switzerland) and Marco Marino (Biozentrum, University of Basel, Switzerland) with the modelling of epitopes on actin structures. We thank Masahika Harata (Tohoku University, Japan) for sequence comparison of epitopes with nuclear Arps and Vesna Oliveri (Biozentrum, University of Basel) for technical assistance with electron microscopy. This work was supported by grants from the Deutsche Forschungsgemeinschaft (to BMJ), the Swiss National Science Foundation (to CAS), and the M.E. Müller Foundation of Switzerland.

References

Baschong, W., Suetterlin, R., Laeng, R.H., 2001. Control of autofluorescence of archival formaldehyde-fixed, paraffin-embedded tissue in confocal laser scanning microscopy (CLSM). J. Histochem. Cytochem. 49, 1565–1572.

Bremer, J.W., Busch, H., Yeoman, L.C., 1981. Evidence for a species of nuclear actin distinct from cytoplasmic and muscles actins. Biochemistry 20, 2013–2017.

Bubb, M.R., Govindasamy, L., Yarmola, E.G., Vorobiev, S.M., Almo, S.C., Somasundaram, T., Chapman, M.S., Agbandje-McKenna, M., McKenna, R., 2002. Polylysine induces an antiparallel actin dimer that nucleates filament assembly: crystal structure at 3.5-A resolution. J. Biol. Chem. 277, 20999–31006.

Clark, T.G., Merriam, R.W., 1977. Diffusible and bound actin nuclei of *Xenopus laevis* oocytes. Cell 12, 883–891.

Clarkson, E., Costa, C.F., Machesky, L.M., 2004. Congenital myopathies: diseases of the actin cytoskeleton. J. Pathol. 204, 407–417.

Dreger, C.K., Konig, A.R., Spring, H., Lichter, P., Herrmann, H., 2002. Investigation of nuclear architecture with a domain-presenting expression system. J. Struct. Biol. 140, 100–115.

Egly, J.M., Miyamoto, N.G., Moncollin, V., Chambon, P., 1984. Is actin a transcription initiation factor for RNA polymerase B? EMBO J. 3, 2363–2371.

Elzinga, M., Phelan, J.J., 1984. F-actin is intermolecularly crosslinked by *N*,*N*′-*p*-phenylenedimaleimide through lysine-191 and cysteine-374. Proc. Natl. Acad. Sci. USA 81, 6599–6602.

Fahrenkrog, B., Aebi, U., 2003. The nuclear pore complex: nucleocytoplasmic transport and beyond. Nat. Rev. Mol. Cell. Biol. 4, 757–766.

Frank, R., 2002. The SPOT-synthesis technique. Synthetic peptide arrays on membrane supports—principles and applications. J. Immunol. Methods 267, 13–26.

Goebel, H.H., Warlo, I.A., 2001. Surplus protein myopathies. Neuromuscul. Disord. 11, 3–6.

Gonsior, S.M., Platz, S., Buchmeier, S., Scheer, U., Jockusch, B.M., Hinssen, H., 1999. Conformational difference between nuclear and cytoplasmic actin as detected by a monoclonal antibody. J. Cell Sci. 112 (Pt. 6), 797–809.

Grenklo, S., Johansson, T., Bertilson, L., Karlsson, R., 2004. Anti-actin antibodies generated against profilin:actin distinguish between non-filamentous and filamentous actin, and label cultured cells in a dotted pattern. Eur. J. Cell Biol. 83, 413–423.

Hofmann, W., Reichart, B., Ewald, A., Muller, E., Schmitt, I., Stauber, R.H., Lottspeich, F., Jockusch, B.M., Scheer, U., Hauber, J., Dabauvalle, M.C., 2001. Cofactor requirements for nuclear export of Rev response element (RRE)- and constitutive transport element (CTE)-containing retroviral RNAs. An unexpected role for actin. J. Cell Biol. 152, 895–910.

Hofmann, W.A., Stojiljkovic, L., Fuchsova, B., Vargas, G.M., Mavrommatis, E., Philimonenko, V., Kysela, K., Goodrich, J.A., Lessard, J.L., Hope, T.J., Hozak, P., de Lanerolle, P., 2004. Actin is part of pre-initiation complexes and is necessary for transcription by RNA polymerase II. Nat. Cell Biol. 6, 1094–1101.

Holmes, K.C., Popp, D., Gebhard, W., Kabsch, W., 1990. Atomic model of the actin filament. Nature 347, 44–49.

Hu, P., Wu, S., Hernandez, N., 2004. A role for beta-actin in RNA polymerase III transcription. Genes Dev. 18, 3010–3015.

Jockusch, B.M., Becker, M., Hindennach, I., Jockusch, H., 1974. Slime mould actin: homology to vertebrate actin and presence in the nucleus. Exp. Cell Res. 89, 241–246.

Kabsch, W., Mannherz, H.G., Suck, D., Pai, E.F., Holmes, K.C., 1990. Atomic structure of the actin:DNase I complex. Nature 347, 37–44.

Kato, M., Sasaki, M., Mizuno, S., Harata, M., 2001. Novel actin-related proteins in vertebrates: similarities of structure and expression pattern to Arp6 localized on *Drosophila* heterochromatin. Gene 268, 133–140.

Kiseleva, E., Drummond, S.P., Goldberg, M.W., Rutherford, S.A., Allen, T.D., Wilson, K.L., 2004. Actin- and protein-4.1-containing filaments link nuclear pore complexes to subnuclear organelles in *Xenopus* oocyte nuclei. J. Cell Sci. 117, 2481–2490.

Kukalev, A., Nord, Y., Palmberg, C., Bergman, T., Percipalle, P., 2005. Actin and hnRNP U cooperate for productive transcription by RNA polymerase II. Nat. Struct. Mol. Biol. 12, 238–244.

Leavitt, J., Gunning, P., Kedes, L., Jariwalla, R., 1985. Smooth muscle alpha-action is a transformation-sensitive marker for mouse NIH 3T3 and Rat-2 cells. Nature 316, 840–842.

Lorenz, M., Popp, D., Holmes, K.C., 1993. Refinement of the F-actin model against X-ray fiber diffraction data by the use of a directed mutation algorithm. J. Mol. Biol. 234, 826–836.

Mayboroda, O., Schluter, K., Jockusch, B.M., 1997. Differential colocalization of profilin with microfilaments in PtK2 cells. Cell Motil. Cytoskeleton 37, 166–177.

Millonig, R., Salvo, H., Aebi, U., 1988. Probing actin polymerization by intermolecular cross-linking. J. Cell Biol. 106, 785–796.

Mockrin, S.C., Korn, E.D., 1981. Isolation and characterization of covalently cross-linked actin dimer. J. Biol. Chem. 256, 8228–8233.

Morton, W.M., Ayscough, K.R., McLaughlin, P.J., 2000. Latrunculin alters the actin-monomer subunit interface to prevent polymerization. Nat. Cell Biol. 2, 376–378.

Nishida, E., Iida, K., Yonezawa, N., Koyasu, S., Yahara, I., Sakai, H., 1987. Cofilin is a component of intranuclear and cytoplasmic actin rods induced in cultured cells. Proc. Natl. Acad. Sci. USA 84, 5262–5266.

Olave, I.A., Reck-Peterson, S.L., Crabtree, G.R., 2002. Nuclear actin and actin-related proteins in chromatin remodeling. Annu. Rev. Biochem. 71, 755–781.

Pendleton, A., Pope, B., Weeds, A., Koffer, A., 2003. Latrunculin B or ATP depletion induces cofilin-dependent translocation of actin into nuclei of mast cells. J. Biol. Chem. 278, 14394–14400.

Percipalle, P., Fomproix, N., Kylberg, K., Miralles, F., Bjorkroth, B., Daneholt, B., Visa, N., 2003. An actin-ribonucleoprotein interaction is involved in transcription by RNA polymerase II. Proc. Natl. Acad. Sci. USA 100, 6475–6480.

Percipalle, P., Jonsson, A., Nashchekin, D., Karlsson, C., Bergman, T., Guialis, A., Daneholt, B., 2002. Nuclear actin is associated with a specific subset of hnRNP A/B-type proteins. Nucleic Acids Res. 30, 1725–1734.

Philimonenko, V.V., Zhao, J., Iben, S., Dingova, H., Kysela, K., Kahle, M., Zentgraf, H., Hofmann, W.A., de Lanerolle, P., Hozak, P., Grummt, I., 2004. Nuclear actin and myosin I are required for RNA polymerase I transcription. Nat. Cell Biol. 6, 1165–1172.

Rando, O.J., Zhao, K., Crabtree, GR., 2000. Searching for a function for nuclear actin. Trends Cell Biol. 10, 92–97.

Reutzel, R., Yoshioka, C., Govindasamy, L., Yarmola, E.G., Agbandje-McKenna, M., Bubb, M.R., McKenna, R., 2004. Actin crystal dynamics: structural implications for F-actin nucleation, polymerization, and branching mediated by the anti-parallel dimer. J. Struct. Biol. 146, 291–301.

Sahlas, D.J., Milankov, K., Park, P.C., De Boni, U., 1993. Distribution of snRNPs, splicing factor SC-35 and actin in interphase nuclei: immunocytochemical evidence for differential distribution during changes in functional states. J. Cell Sci. 105 (Pt. 2), 347–357.

Sameshima, M., Chijiiwa, Y., Kishi, Y., Hashimoto, Y., 1994. Novel actin rods appeared in spores of *Dictyostelium discoideum*. Cell Struct. Funct. 19, 189–194.

Sameshima, M., Kishi, Y., Osumi, M., Minamikawa-Tachino, R., Mahadeo, D., Cotter, DA., 2001. The formation of actin rods composed of actin tubules in *Dictyostelium discoideum* spores. J. Struct. Biol. 136, 7–19.

Sanger, J.W., Sanger, J.M., Kreis, T.E., Jockusch, B.M., 1980. Reversible translocation of cytoplasmic actin into the nucleus caused by dimethyl sulfoxide. Proc. Natl. Acad. Sci. USA 77, 5268–5272.

Scheer, U., Hinssen, H., Franke, W.W., Jockusch, BM., 1984. Microinjection of actin-binding proteins and actin antibodies demonstrates involvement of nuclear actin in transcription of lampbrush chromosomes. Cell 39, 111–122.

Schutt, C.E., Myslik, J.C., Rozycki, M.D., Goonesekere, N.C., Lindberg, U., 1993. The structure of crystalline profilin-beta-actin. Nature 365, 810–816.

Small, J.V., Celis, J.E., 1978. Direct visualization of the 10-nm (100-A)-filament network in whole and enucleated cultured cells. J. Cell Sci. 31, 393–409.

Smith, S.S., Kelly, K.H., Jockusch, B.M., 1979. Actin co-purifies with RNA polymerase II. Biochem. Biophys. Res. Commun. 86, 161–166.

Stüven, T., Hartmann, E., Gorlich, D., 2003. Exportin 6: a novel nuclear export receptor that is specific for profilin.actin complexes. EMBO J. 22, 5928–5940.

Wada, A., Fukuda, M., Mishima, M., Nishida, E., 1998. Nuclear export of actin: a novel mechanism regulating the subcellular localization of a major cytoskeletal protein. EMBO J. 17, 1635–1641.

Welch, W.J., Suhan, J.P., 1985. Morphological study of the mammalian stress response: characterization of changes in cytoplasmic organelles, cytoskeleton, and nucleoli, and appearance of intranuclear actin filaments in rat fibroblasts after heat-shock treatment. J. Cell Biol. 101, 1198–1211.

Yahara, I., Aizawa, H., Moriyama, K., Iida, K., Yonezawa, N., Nishida, E., Hatanaka, H., Inagaki, F., 1996. A role of cofilin/destrin in reorganization of actin cytoskeleton in response to stresses and cell stimuli. Cell Struct. Funct. 21, 421–424.